Journal of Interfaces, Thin films, and Low dimensional systems 2 (2) Winter and Spring (2019) 167-175

Three-dimensional calculations of the magnetic fields in a finite superconducting hollow cylinder in an applied axial magnetic field

Batool Mohammadzadeh-Dehsorkh

Department of Physics, Faculty of Science, University of Qom, Qom 3716146611, Iran

ARTICLE INFO

Article history:
Received 13 January 2019
Revised 9 December 2019
Accepted 25 March 2020
Available online 12 April 2020

Keywords:
Superconductivity
Hollow cylinder
Magnetic Field
Critical state model

ABSTRACT

In this study, a set of self-consistent coupled-integral equations for the local magnetic flux and current distributions in a finite superconducting hollow cylinder under an axial magnetic field has been directly derived by using the Biot-Savart law within the framework of the critical-state model. The equations were first solved numerically in the three-dimensional space before obtaining the hysteresis loops for the Kim and Exponential models. We have assumed the contribution of the flux penetration from the inner surface of the sample to be higher than that of other surfaces. It is found that the variation in the area of lateral surface changes the magnitude of the magnetic moment of the finite hollow cylinder in the applied magnetic field. The obtained results are in good agreement with calculates. The formalism presented here can be used for an arbitrary shape of the superconducting system in the presence of any magnetic field dependence of the critical current density $J_c(B)$ in an external magnetic field of arbitrary direction.

1 Introduction

Recently, various properties of high-temperature superconductors (HTS) have resulted in the appearance of vast application areas. Depending on applications or fundamental properties, HTSCs have been considered as bulk thin films. The sensitive magnetometers, e.g. scanning superconducting quantum interference device (SQUIDs) are very important for the investigation of the magnetic flux, flux penetration, current density distributions, and non-destructive measurement in thin films [1, 2]. The bulk materials are useful for shielding purposes [3-6] for instance fusion reactor containment vessels, large magnets [7], nuclear magnetic resonance (NMR) devices, and electronic applications [8-10].

According to Maxwell equations ($\vec{\nabla} \times \vec{B} = \mu_0 \vec{J}$), when an external magnetic field is applied, the induced shielding current flows in the direction perpendicular to the external magnetic field, so-called as the screening current. When the applied field is not sufficiently strong, the internal magnetic flux density ($\vec{B}$) of the superconductor will be zero, and screening currents will flow in a certain distance of the surface called the penetration depth. This is while when a sufficiently strong magnetic field is applied, the current density penetrates throughout the sample which prevents the internal field to be zero. This situation and the corresponding current density are

*Corresponding author.
Email address: Batoolmohammadzadeh@Yahoo.com
DOI: 10.22051/jitl.2020.24074.1024

respectively regard as a critical state and a critical current density [11].

Studies regarding the magnetic behavior of high-T_c superconductors have shown that the critical current density, $J_c(B)$, depends intensively on the local flux density ($\overrightarrow{B}$) [12]. The critical state models (CSMs), introduced by Bean [13] and Kim et al. [14], were found to be powerful tools for studying superconducting properties. Bean's model is based on the assumption in which the critical current density (J_c) is independent of $\vec{B}$, while in other models, it is assumed that J_c depends on the local flux density. $J_c(B)$ in Kim's model is given as

$$J_c(B) = J_c /(1+\left|B(\vec{r})\right|/ B_k), \quad (1)$$

where B_k is the scaling field while J_c is the Kim's critical current density. We suppose $B_k = 1$ throughout the calculations.

The exponential model expresses the relevance of flux and critical density as

$$J_c(B) = J_c \exp(-\left|B(\vec{r})\right|/ B_k) \ . \quad (2)$$

The magnetic moment of a superconductor is given by

$$\vec{m} = \frac{1}{2}\int_V [\vec{r}' \times \vec{J}(r')]\, d^3 r'. \quad (3)$$

The magnetization (M), which can be calculated via $\overrightarrow{M} = \vec{m}/V$ (V; the sample volume), is an irreversible property in superconductors. In other words, when the applied magnetic field reaches the initial value, the system does not reset to its virgin state; and thus, the hysteretic effects occur. In addition, magnetization determines the volume of flux which is penetrated by the induced shielding currents [15, 16].

The macroscopic behavior of superconducting slabs [17-20], disks [16, 19-20], spheres [21], and cylinders [16, 20-25] in parallel and axial fields have been investigated by using critical state models. Brandt [16, 24-25] used the critical models for circular disks, long and finite cylinders, and ring samples in a perpendicular magnetic field. Zeldov et al. [17] have studied an infinitely long thin film strip. Zhu et al. [19] also used the disk-shaped thin film. Babaei et al. [26] studied a current-carrying superconducting Corbino disk. McDonald et al. [27] and Clem [28] studied a critical state model for the nonlinear ac response of a superconducting coaxial-type transmission line. They considered a sample where the outer conductor was a superconducting cylindrical shell while the inner conductor was a superconducting wire of elliptical or rectangular shape. By employing a simple circuital model and considering the mutual coefficient between the circuits representing the current loops in the system, Luca [29] also studied the field-cooled magnetic behavior of type-I superconducting cylinders consisting of one or two holes. Araujo-Moreira et al. [30] and Sanchez et al. [31] have presented a model to understand the current flow and field penetration in finite type-II superconducting cylinders. Douglass [32] and Arutunian et al. [33-34] derived the Gibbs energy and order parameter for a thin hollow superconducting cylinder via the Ginzburg-Landau theory. Masale et al. [35] and Yampolskii et al. [36] have also investigated the effective radius of mesoscopic superconducting hollow cylinders in the range of validity of phenomenological Ginzburg-Landau theory. The Gibbs free energy calculations for superconductors are useful to study the thermo-dynamical properties and phenomenological studies. In another attempt, some researchers have numerically calculated the superconducting properties of a finite superconducting tube by using the Bean model [37]. Sheha et al. [38] have obtained the curved flux line effects in a type-II superconducting hollow cylinder when an external magnetic field was applied inside the hollow region. Alqadi and his co-researchers have analyzed the interaction between a cylindrical magnet and a superconducting hollow cylinder in the Meissner state by using the dipole–dipole model [39]. Altshuler et al. [40] calculated the free energy in a superconducting hollow cylinder by considering the penetration of circular vortices. Additionally, in another work [41], they utilized Bean's and Kim's models to a type II superconducting hollow cylinder in the presence of a current-carrying coaxial wire. Fagnard et al. [42] have studied the magnetic shielding behavior of superconducting hollow cylinders both experimentally and theoretically by using a nonlinear $E(J)$ constitutive model in Kim with negative power laws. In another work [43], they studied a finite superconducting hollow cylinder having two slits in a vertical plane along a diameter. Frankel [44] also developed a model for flux trapping by superconducting tubular samples

in transverse fields. Holguin et al. [45] have prepared a superconducting hollow cylinder and measured its magnetic flux. They found that the magnetic field penetrates throughout the sample and reaches the hole after a time delay.

Based on the aforementioned results obtained by other researchers, we studied the induced magnetic field, current density distributions, and magnetization hysteresis loops for a finite 3-D hollow cylinder located in an applied axial magnetic field in the absence of a transport current. For this purpose, we used a numerical 3-D standard model by means of three critical state models. This method is based on the numerical solution of a series of self-consistency coupled-integral equations to determine the current density, J_c, inside the superconductor.

The outline of this study is as follows. In Section 2, we present three-coupled integral equations for the three components of the magnetic flux density by implementing the Biot-Savart law in the external magnetic field. This is repeated for the Bean, Kim, and exponential models to obtain the dependence between the local magnetic field and the radial coordinate in a different external magnetic fields. In Section 3, the magnetization hysteresis loops are calculated for the aforementioned models. Section 4 presents the results and discussions. The conclusion is given in Section 5.

2 Magnetic field profiles and current density in a superconducting hollow cylinder

We considered a superconducting hollow cylinder with an inner radius of R_1, an outer radius of R_2, with height of L. We have Assumed $L > R_2 - R_1 \gg \lambda$, where λ is the London penetration depth. The parameters R_2 and L are taken smaller than the 2-D screening length [17]. The origin of the coordinate system is at the center of the hollow cylinder so that the cylinder axis will be parallel to the +z-axis, see Fig. 1. By employing a uniform external magnetic field (B_a) in a zero-field-cooled hollow superconducting cylinder, the induced shielding current will flow azimuthally. If B_a is assumed to be large, the magnetic flux penetrates through the hollow cylinder and its hole.

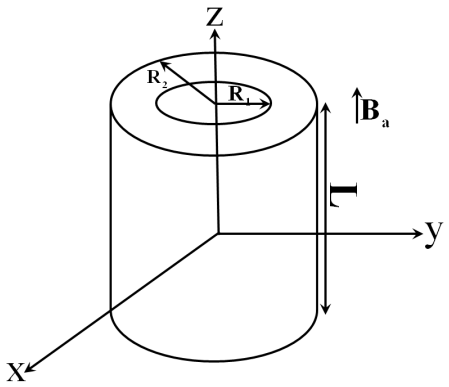

Figure 1. Schematic of a finite superconducting hollow cylinder in a parallel applied magnetic field.

However, the three components of the magnetic flux density in reduced units can be calculated by using the Bio-Savart law as

$$\frac{B_i}{B_c} = \oint_V \frac{dV' J f_i(\vec{r},\vec{r}')}{\left(\sqrt{P(\vec{r},\vec{r}')}\right)^3}, \tag{4}$$

where i = ρ, φ, z, $B_c = \mu_0 J_c R_2^2/4\pi$, $J(\vec{r}) = J_c(\vec{r})/J_c$. This is while $J_c(\vec{r})$ represents the current density in the azimuthal direction with J_c possessing a constant value. We write

$$f_\rho(\vec{r},\vec{r}') = \cos(\varphi' - \varphi)(z' - z), \tag{5}$$

$$f_\varphi(\vec{r},\vec{r}') = \sin(\varphi' - \varphi)(z' - z), \tag{6}$$

$$f_z(\vec{r},\vec{r}') = \rho' - \rho\sin(\varphi' - \varphi), \tag{7}$$

$$P(\vec{r},\vec{r}') = \rho^2 + \rho'^2 - 2\rho\rho'\cos(\varphi' - \varphi) + (z' - z)^2. \tag{8}$$

By substituting Eqs. (5)-(8) in Eq. (4), we obtain a system of three self-consistent integral equations that can be solved numerically by the Newton's method. According to Newton's method, the equations can be written as $B_i = 0$. Initially, we estimate a solution point, r_0, for $B_i(r) = 0$ in where i = ρ, φ, z before Taylor expanding $B_i(r)$ around the specific point. Thus, we have

$$B_i(r_1) = 0 = B_i(r_0) + (r_1 - r_0)B_i'(r_0). \tag{9}$$

In the next step, we obtain the solution point from

$$r_1 = r_0 - B_i(r_0)/B_i'(r_0)\ . \quad (10)$$

By repeating Eq. (10), we can obtain the real roots of $B_i(r) = 0$ from

$$r_{k+1} = r_k - B_i(r_k)/B_i'(r_k)\ . \quad (11)$$

Finally, the three components of the magnetic flux density are obtained. The critical current density may be determined for Kim and Exponential models by Eqs. (1) and (2). The results obtained from the profiles of the critical current and local flux densities at $z = L/2$ for three magnitudes of the applied magnetic field are shown in Figs. 2 and 3, respectively.

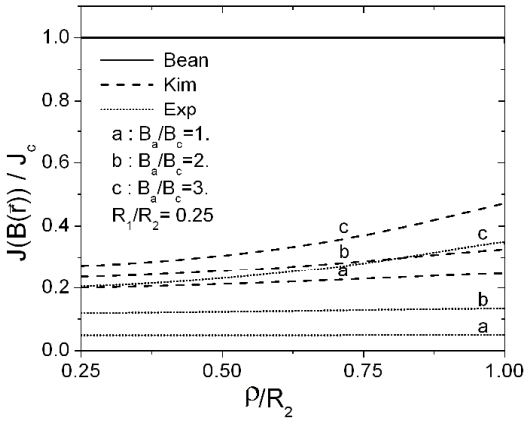

Figure 2. The profiles of critical current densities versus the radial distance at $z = L/2$ for three applied magnetic fields and three different CSM models. Solid, dashed, and dotted lines show results of the Bean, Kim, and Exponential models, respectively.

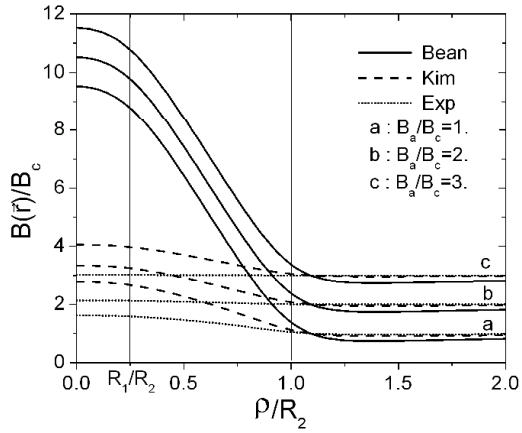

Figure 3. The profiles of total local magnetic flux versus the radial distance at $z = L/2$ for three applied magnetic fields and three different CSM models. Solid, dashed and dotted lines show the results of the Bean, Kim, and Exponential models, respectively.

3 Magnetization and hysteresis loop

In this section, we obtain the magnetization and hysteresis loops in accordance with the resulting profiles for critical current and local flux densities for the Bean, Kim, and Exponential models. The three components of magnetization regarding the sample can be determined according to Eqs. (12)-(14):

$$\frac{M_\rho}{M_c} = -\frac{1}{2V}\oint_V dV' z' J(\vec{r}'), \quad (12)$$

$$\frac{M_\varphi}{M_c} = 0, \quad (13)$$

$$\frac{M_z}{M_c} = \frac{1}{2V}\oint_V dV' \rho' J(\vec{r}'), \quad (14)$$

with

$$M_c = \left(\frac{\pi J_c}{V}\right)\sqrt{\left(\frac{(R_2^2 - R_1^2)L^2}{4}\right)^2 + \left(\frac{(R_2^3 - R_1^3)L}{3}\right)^2}$$

where we have

$$\mathbf{M}(B_a, J_c) = \sqrt{\frac{M_\rho^2 + M_\varphi^2 + M_z^2}{M_c^2}}\ . \quad (15)$$

In order to obtain the hysteresis loops, we initially calculate the negative magnetization, $M_\downarrow(B_a, J_c)$, by decreasing the applied magnetic field from $+B_0$ to $-B_0$ before calculating $M_\uparrow(B_a, J_c)$ by increasing the applied magnetic field from $-B_0$ to $+B_0$. As explained by Zhu et al. [19], when B_a varies from B_0 to 0, the critical current and flux densities are respectively represented by J_c and B_0. However, these parameters can be substituted by $2J_c$ and $B_0 - B_a$ when B_a decreases from 0 to $-B_0$. As a result, the general expression for the negative magnetization is:

$$\mathbf{M}_\downarrow(B_a, J_c) = \mathbf{M}(B_a, J_c) - \mathbf{M}(B_0 - B_a, 2J_c), \quad (16)$$

In the increasing range of B_a, magnetization will be calculated according to

$$\mathbf{M}_{\uparrow}(B_a, J_c) = -\mathbf{M}_{\downarrow}(-B_a, J_c). \quad (17)$$

The virgin state of magnetization can be evaluated by increasing the applied field from 0 to $+B_0$. In general, the magnetization hysteresis loops can be obtained as follows: initially, we vary B_a from $-B_0$ to $+B_0$ or vice versa before calculating the components of the local flux density via Eqs. (4)-(8) by following the algorithms explained in Section 2. By implementing these components and Eq. (15), the magnetic flux distribution when the external magnetic field varies from $-B_0$ to $+B_0$ is calculated. It is worth noting that B_0 is the maximum value that B_a is able to gain. The obtained results are shown in Figure 4. Subsequently, we used the components of the local flux density in Eqs. (12)-(14) and calculated the components of magnetization for various values of B_a. The initial magnetization could be calculated by Eq. (15).

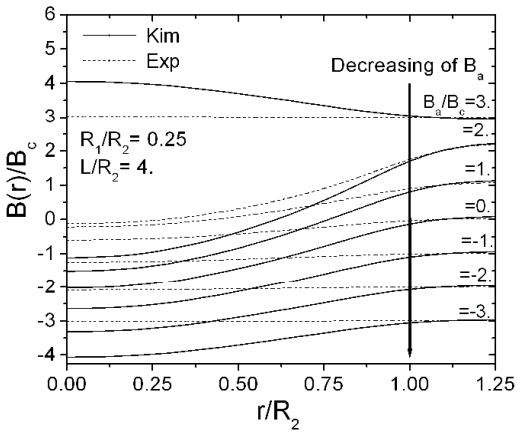

Figure 4. The profiles of total local magnetic flux versus the radial distance in normalized units as the applied magnetic field B_a/B_c is reduced from 3 to -3. Solid and dashed lines show the results of Kim's and Exponential models, respectively. The arrows indicate the decreasing direction of B_0.

The magnetization hysteresis loops of the sample implemented in the Kim and Exponential models were obtained by using the initial magnetization in Eqs. (17)-(18). On the whole, all the calculations were carried out using the Fortran program where the results have been presented in Figure 5.

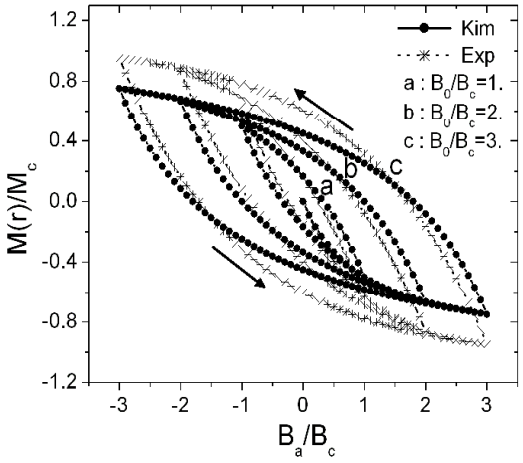

Figure 5. The magnetization hysteresis loops of Kim's and Exponential models at three applied magnetic fields in reduced units for B_a/B_c. The circular and star symbols show the results of Kim's and Exponential models, respectively. The arrows indicate the increasing direction of B_0.

4 Results and discussion

As seen in Figure 2, the normalized critical current densities for the Kim and Exponential models are generally smaller than those of Bean's model. In addition, it can be observed that the local field dependency of J_c is significant for the Kim and Exponential models, especially when $B_a > 2B_c$, see curves "c" in Figure 2. The critical current density reaches a maximum value at the outer surface and a minimum at the inner surface.

We assumed that the flux starts to penetrate from the inner lateral surface of the sample and the shielding currents flow inside the sample, generating a magnetic field within the hole, see Figure 3. In addition, the flux will reach a maximum value in the middle of the sample ($B(r=0) > B_a$) due to easy penetration of the flux into the hole without encountering a trap. These results are consistent with Lousberg et al's [37]. Also, it can be seen from Figure 3 that the flux density reduces from 0 to R_2 because the positive applied field is constant all over the surface; however, the negative magnetic field is induced by the increasing shielding current.

Increasing the exerted magnetic field causes an increase in flux penetration from the inner surface into the superconducting body so that the whole field

profile is mainly shifted upwards, and the total behavior of the local magnetic field remains unchanged. The similar results were reported by Lousberg et al [37].

Figure 4 shows that the magnetic flux distribution varies for different histories of the external condition due to the irreversible behavior of the superconductors.

Figure 5 shows that the peaks are situated at negative B_a on the downward branches of the major loops for both dependence models of $J_c(B)$, Kim's and Exponential, due to the fact that the geometry considered in this study is parallel, similar to Karmakar's [46]. It is clear from the figure that by increasing the applied magnetic field, the penetrated volume of super-currents increases. The magnetic susceptibility in Exponential model is higher than that of Kim's model showing that the volume penetrated by the induced super-currents in Exponential model is higher than that of the Kim model. In accordance with Brandt's results [24], it can be stated that the obtained finding is the result of the saturation value of m depending on the ramp rate of B_a. Therefore, when the applied magnetic field is higher than that of full penetration, the relative variations of $B(r)$ becomes small compared to the average value of B, and approximately equal B_a.

The results of the magnetic moment versus the applied magnetic field are shown in Figure 6 for a given R_1 at three different values of L/R_2. It is evident that the magnitude of magnetic moment decreases when the height of the cylinder increases in Kim and Exponential models. The results show that the area of lateral surface has an effect on the magnitude of magnetic moment of the sample. For a finite hollow cylinder, the flux lines spread out close to the outer surface because of the demagnetization effects. Consequently, the shielding currents flow in an expanded region at the periphery of the superconductor. The obtained results are the same as those obtained experimentally by Fagnard et al. [47] and Denis et al. [48-49].

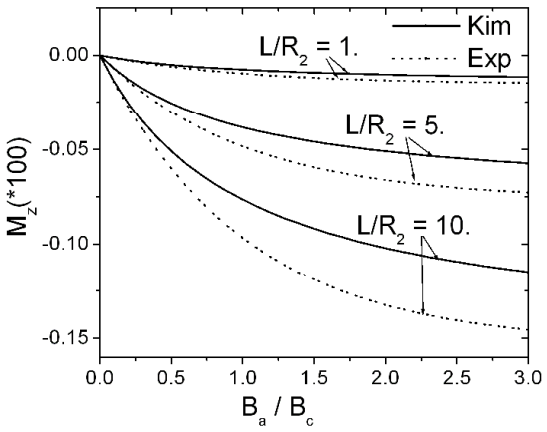

Figure 6. The results of magnetic moment component versus the applied magnetic field for Kim's and Exponential models at three different ratios of L/R_2 equalt to 1, 5, and 10. Solid and dotted lines indicate the results of Kim's and Exponential models.

5 Conclusions

In this study, we studied the magnetic behavior of a finite superconducting hollow cylinder in an external magnetic field within the framework of the critical state models. We carried out all the calculations in 3-D coordinates and presented a numerical method for calculating the local magnetic flux, current density distributions, and magnetization hysteresis loops in a superconducting sample. We obtained all the results in the absence of a vector potential, $A(\overrightarrow{r})$, or the Green's function, indicating that the method used in this study is much more accurate than taking the numerical derivative of the mentioned methods. It was concluded that the local flux and current density profiles are both sensitive to the $J_c(B)$ dependent models. We found that the field profile depends on the value of the applied magnetic field; however, the total behavior of the local magnetic field did not change. By changing the applied magnetic field, the dependency of the magnetic flux distribution on the histories of the external condition was seen for superconductors. In addition, the results revealed that the area of the lateral surface affected the magnitude of the magnetic moment. We believe that the calculations used in this study can be useful to study the features of superconductors having arbitrary shapes in an external magnetic field.

References

[1] H. H. Qi, P. L. Lang , M. J. Zhang, T. S. Wang, D. N. Zheng and Y. J. Tian, "High-T_c dc-SQUID magnetometer and its application in eddy current non-destructive evaluation", Cryogenics **44** (2004) 695.

[2] D. Winkler, "Superconducting analogue electronics for research and industry", Superconductivity Science and Technology **16** (2003) 1583.

[3] H. Altenburg, J. Plewa, W. Jaszczuk, M. Itoh, I. Brunets, A. Buev, and T. Vilics, "Superconducting materials for electronic applications", Physica C: Superconductivity **1046** (2002) 372.

[4] S. H. Lee, J. S. Jeong, K. T. Jung, J. P. Hong, and Y. S. Jo, "Advanced 3-Dimensional Magnetic Field Analysis of Superconducting Machines Using Analytical Method", IEEE Transactions on Applied Superconductivity **23** (2013) 4900704.

[5] T. Matsushita, "Current high-temperature superconducting coils and applications in Japan", Superconductivity Science and Technology **13** (2000) 51.

[6] D. Hechtfischer, "Generation of homogeneous magnetic fields within closed superconductive shields", Cryogenics **27** (1987) 503.

[7] L. Rossi, "Superconductivity: its role, its success and its setbacks in the Large Hadron Collider of CERN", Superconductivity Science and Technology **23** (2010) 034001.

[8] P. Tixador, X. Obradors, R. Tournier, T. Puig, D. Bourgault, X. Granados, J. M. Duval, E. endoza, X. Chaud, E. Varesi, E. Beaugnon, and D. Isfort, "Quench in bulk HTS materials-application to the fault current limiter", Superconductivity Science and Technology **13** (2000) 493.

[9] J. Leveque and A. Rezzoug, "A new kind of superconducting current limiter", Superconductivity Science and Technology **15** (2002) 630.

[10] N. Christofield, D. N. Sobieski, J. C. Erker, S. May, and M. P. Augustine, "A single coil radio frequency gradient probe for nuclear magneticresonance applications", Review of Scientific Instruments **83** (2012) 124701.

[11] Ch P. Poole, J. Horacio, A. F. Richard, J. Creswick, and R. Prozorov, "superconductivity", Netherlands : Academic Press (2007).

[12] P. N. Mikheenko and Yu E. Kuzovlev, "Inductance measurements of HTSC films with high critical currents", Physica C: Superconductivity **204** (1993) 229.

[13] C. P. Bean, "Magnetization of hard superconductors", Physical Review Letters **8** (1962) 250.

[14] Y. B. Kim, C. F. Hempstead, and A. R. Strnad, "Critical persistent currents in hard superconductors", Physical Review Letters **9** (1962) 306.

[15] D. X. Chen and A. Sanchez, "Magnetic properties of High-Tc superconducting grains", Physical Review B **45** (1992) 10793.

[16] E. H. Brandt, "Susceptibility of superconductor disks and rings with and without flux creep", Physical. Review B **55** (1997) 14513.

[17] E.Zeldov, J.R.Clem, M.McElfresh and M.Darwin, "Magnetization and transport currents in thin superconducting films", Physical Review B **49** (1994) 9802.

[18] A. Klein and A. Godunov, "Introductory computational physics", Cambridge: University Press, (2006).

[19] J. Zhu, J. Mester, J. Lockhart, and J. Turneaure, "Critical states in 2D disk-shaped type-II superconductord in periodic external magnetic field", Physica C: Superconductivity **212** (1993) 216.

[20] D. V. Shantsev, Y. M. Galperin, and T. H. Johansen, "Thin superconducting disk with field-dependent critical current: Magnetization and ac susceptibilities", Physical Review B **61** (2000) 9699.

[21] R. Navarro and L. J. Campbell, "Magnetic-fiux profiles of high-T, superconducting granules: Three-dimensional critical-state-model approximation", Physical Review B **44** (1991) 10146.

[22] T. H. Johansen and H. Bratsberg, "Critical-state magnetization of type-11 superconductors in rectangular slab and cylinder geometries", Journal of Applied Physics **77** (1995) 3945.

[23] M. W. Coffey, "Pancake vortex in a superconducting cylinder", Physical Review B **51** (1995) 15600.

[24] E. H. Brandt, "Superconductor disks and cylinders in an axial magnetic field: I. Flux penetration and magnetization curves", Physical Review B **58** (1997) 6506.

[25] E. H. Brandt, "Superconductor disks and cylinders in an axial magnetic field: II. Nonlinear and linear ac susceptibilities", Physical Review B **58** (1997) 6523.

[26] A. A. B. Brojeny and J. R. Clem, "Magnetization of a current-carrying superconducting Corbino disk", Physical Review B **64** (2001) 184507.

[27] J. McDonald, J. R. Clem, and D. E. Oates, "Critical-state model for harmonic generation in a superconducting microwave resonator", Physical Review B **55** (1997) 11823.

[28] J. R. Clem, "Theory of flux cutting and flux transport at the critical current of a type-II superconducting cylindrical wire", Physical Review B **83** (2011) 214511.

[29] R. D. Luca, "Positive Field-Cooled Susceptibility in Multiply Connected Type-I Superconductors", Journal of Modern Physics **4** (2013) 5.

[30] F. M. A. Moreira, C. Navau, and A. Sanchez, "Meissner state in finite superconducting cylinders with uniform applied magnetics field", Physical Review B **61** (2000) 634.

[31] A. Sanchez and C. Navau, "Magnetic properties of finite superconducting cylinders. I. Uniform applied field", Physical Review B **64** (2001) 214506.

[32] D. H. Douglass, "Properties of a Thin Hollow Superconducting Cylinder", Physical Review **132** (1963) 513.

[33] R. M. Arutyunyan, V. L. Ginzburg, and G. F. Zharkov, "Magnetic vortices and thermoelectric effect in a hollow superconducting cylinder", JETP **84** (1997) 1186.

[34] R. M. Arutunian and G. F. Zharkov, "Behavior of a Hollow Superconducting Cylinder in a Magnetic Field", Journal of Low Temperature Physics **52** (1983) 409.

[35] M. Masale, N. C. Constantinou and D R Tilley, "The critical field of a hollow type-II superconducting cylinder", Superconductivity Science and Technology **8** (1993) 287.

[36] S. V. Yampolskii, F M Peeters, B J Baelus and H J Fink, "Effective radius of superconducting rings and hollow cylinders", Physical Review B **64** (2001) 3945.

[37] G. P. Lousberg, M. Ausloos, Ch Geuzaine, P. Dular, Ph Vanderbemden, and B. Vanderheyden, "Numerical simulation of the magnetization of high-temperature superconductors: a 3D finite element method using a single time-step iteration", Superconductivity Science and Technology **22** (2009) 055005.

[38] L. N. Shehata and H. T. F. Refai, "Curved Flux Line Effects in a Type-I1 Superconducting Hollow Cylinder", physica status solidi **133** (1986) 707.

[39] M. K. Alqadi, F. Y. Alzoubi, S. M. Saadeh, H. M. AlKhateeb, and N. Y. Ayoub, "Force Analysis of a Permanent Magnet and a Superconducting Hollow Cylinder", Journal of Superconductivity and Novel Magnetism **25** (2012) 1469.

[40] E. Altshuler and R. Mulet , "Penetration of Circular Vortices into a Superconducting Hollow Cylinder", Journal of Superconductivity **8** (1995) 779.

[41] E. Altshuler and R. Mulet, "The azimuthal critical state of a superconducting hollow cylinder", Physica C **292** (1997) 39.

[42] J. F. Fagnard, M. Dirickx, M. Ausloos, G. Lousberg, B. Vanderheyden and Ph Vanderbemden, "Magnetic shielding properties of high- Tc superconducting hollow cylinders: model combining experimental data for axial and transverse magnetic field configurations", Superconductivity Science and Technology **22** (2009) 105002.

[43] J. F. Fagnard, S. Elschner, A. Hobl, J. Bock, B. Vanderheyden, and P. Vanderbemden, "Magnetic shielding properties of a superconducting hollow cylinder containing slits: modelling and experiment", Superconductivity Science and Technology **25** (2012) 104006.

[44] D. J. Frankel, "Model for flux trapping and shielding by tubular superconducting samples in

transverse fields", IEEE Transactions on Magnetics **15** (1979) 1349.

[45] E. Holguin, H. Berger, and J. F. Loude, "Dynamics of flux penetration in superconducting YBaCuO Hollow Cylinder", Solid State Communications **74** (1990) 263.

[46] D. Karmakar, "Studies of magnetization and related properties for hard type-II superconductors", Indian Journal of Physics **79** (2005) 1107.

[47] J. F. Fagnard, S. Denis, G. Lousberg, M. Dirickx, M. Ausloos, B. Vanderheyden and Ph Vanderbemden, "DC and AC Shielding Properties of Bulk High-Tc superconducting Tubes", IEEE Transactions on Applied Superconductivity **19** (2009) 2905.

[48] S. Denis, M. Dirickx, Ph Vanderbemden, M. Ausloos, and B. Vanderheyden, "Field penetration into hard type-II superconducting tubes: effects of a cap, a non- superconducting joint, and non-uniform superconducting properties", Superconductivity Science and Technology **20** (2007) 418.

[49] S. Denis, L. Dusoulier, M. Dirickx, Ph Vanderbemden, R. Cloots, M. Ausloos, and B. Vanderheyden, "Magnetic shielding properties of high-temperature superconducting tubes subjected to axial fields", Superconductivity Science and Technology **20** (2007) 192.